

Skeletal T–O–T Vibrations as a Tool for Characterization of Divalent Cation Complexation in Ferrierite

Zdeněk Sobalík, Zdenka Tvarůžková, and Blanka Wichterlová*

J. Heyrovský Institute of Physical Chemistry, Academy of Sciences of the Czech Republic, Dolejškova 3, CZ-182 23 Prague 8, Czech Republic

Received: April 28, 1997; In Final Form: November 24, 1997

The effect of several divalent cations (Mn^{2+} , Mg^{2+} , Ni^{2+} , and Co^{2+}) exchanged in Na-ferrierite and ammonia adsorption/desorption was studied by FTIR spectroscopy in the range 4000–400 cm^{-1} . The complete cation exchange eliminated zeolite bridging acidic hydroxyls and provided for monitoring of the stretching and bending modes of ammonia interacting with cations and the accompanying parallel changes of the zeolite lattice vibrations induced by bare cations and cation–ligand complexes at various ammonia coverage. Dehydration of ferrierites with ion-exchanged divalent cations gives formation of new IR bands in the transmission window between antisymmetric (around 1070 cm^{-1}) and symmetric (around 780 cm^{-1}) T–O–T stretching lattice modes. These new bands disappear upon full saturation by ammonia and reappear under complete ammonia desorption. They are assigned to antisymmetric stretching T–O–T mode of zeolitic lattice shifted to a lower frequency due to the reversible local deformation of the flexible zeolitic lattice by the interaction with a bare divalent cation (a lower frequency band, B_0) or with a low, probably 1:1 cation–extraframework ligand complex with ammonia molecule (a higher frequency band, B_1). The extent of perturbation of the ferrierite lattice due to a divalent cation is locally partly decreased by formation of such cation–extraframework ligand complex. By taking the position of the T–O–T antisymmetric band of the parent hydrated Na-ferrierite at 1070 cm^{-1} as reference, this relaxation effect, caused by bonding of a guest molecule, was found to amount to about 15–20% of the spectral shift produced by bonding of a bare divalent cation to the framework.

1. Introduction

The high and unique activity of metal ion loaded high silica zeolites (e.g., ZSM-5, ferrierite, beta, and mordenite) in NO decomposition and selective catalytic reduction (SCR) by hydrocarbons^{1,2} and ammonia (see e.g., ref 3) stimulates still increasing interest for establishing parameters controlling the siting and distribution of divalent cations in the zeolite matrices and for providing information on the structure of cation–guest ligand complexes. The standard methods of structural analysis (e.g., XRD), giving plentiful data for cation siting in aluminium rich zeolites,^{4–7} have been met with severe limitations with high silica zeolites because of the low concentration of the metal ions and the low symmetry of the zeolites matrices. Accordingly, there is a sustained need for development and application of alternative sophisticated methods, providing information on the cation siting-coordination within such systems. Recently, a combination of several complementary spectroscopic methods, yielding a multilevel view on the subject, has proven to be highly promising.^{8–13}

The realistic description of cation siting in catalytically relevant systems necessitates the inclusion of cation interactions with reacting molecules as well as, with special importance for reactions of environmental catalysis, with other gas phase components occurring in these systems (e.g., water, CO_2 etc.). This means that the real challenge is to characterize both a bare metal cation (M) siting, its bonding to framework oxygen ligands in a $(\text{Si,Al})\text{O}_n\text{--M}$ complex, and multiligand complexes schematically described as $(\text{Si,Al})\text{O}_n\text{--M--L}_m$, where $(\text{Si,Al})\text{O}_n$

represents a zeolite framework polyoxygen ligand complex and L a guest ligand.

Ion exchange of a “bare” divalent cation (by this is denoted a cation bonded exclusively to the zeolite framework polyoxygen anion ligands) brings about considerable changes in the lattice parameters.^{4–7,14,15} Principally these changes concern T–O bond length and T–O–T angles, and to a lesser extent O–T–O angles, as documented well, e.g., on Co(II) -⁵ and Mn(II) -⁷chabazite (with the framework rich in aluminium) by single-crystal XRD data. The exchange of a bare cation is probably accompanied by a decrease of the electron density on the framework AlO_4 -tetrahedra adjacent to the divalent cation.¹⁶ As shown for several systems, bonding of a guest ligand to the bare cation brings about further modification of the cation–framework interaction (see, e.g., ref 14), resulting in a partial decrease of the framework local deformation. Generally, much smaller effects on the zeolite lattice parameters were found upon ion exchange of a monovalent cation (see, e.g., Cs(I)).⁶

Fourier-transform infrared spectroscopy (FTIR) has already shown high potential for providing information on bare cations located at cationic sites and on gas molecules bonded to the cations. The spectral region 4000–1300 cm^{-1} provides information on the O–H bonds and stretching and bending vibrations of adsorbed molecules. The region between 1300 and 400 cm^{-1} covers the lattice modes of the zeolite framework. Due to limitations of the experimental setup of the presented study at wavenumbers above 400 cm^{-1} , no direct information on cation distribution, expected at the region below 250 cm^{-1} ,¹⁷ could be obtained. The cation ion exchange into the zeolite is reflected

in changes of the vibration modes connected with the TO_4 tetrahedra^{14,17,18} and could thus provide direct evidence on changes of the parameters of the T–O bonding and perturbation of the flexible lattice. The T–O–T antisymmetric and symmetric modes are observed in the spectral regions 1350–850 cm^{-1} and 850–620 cm^{-1} , respectively.¹⁷ In the spectral transmission window between these two spectral modes, usually found for zeolites around 900 cm^{-1} , new spectral bands were observed after high temperature evacuation of divalent metal-exchanged zeolites and assigned to a shifted position of the T–O–T antisymmetric band, resulting from local framework perturbation.^{14,17,19–21} After heating in vacuum of a series of metal exchanged Y zeolites, a band at the transmission window was identified at 931 cm^{-1} for both Co- and Ni-Y, and at 962 cm^{-1} for Cu-Y.¹⁷ (As follows from the discussion in that paper it should be assigned to Cu(I) formed due to autoreduction of Cu(II) during evacuation at high temperature.) Such an experimental approach using FTIR spectroscopy was employed by Sachtler et al.^{19–21} for detection of the reduction of Cu(II) to Cu(I) in ZSM-5. The T–O–T band at 918 cm^{-1} ascribed to the shifted T–O–T antisymmetric mode due to Cu(II) ion exchange was found to move to 965 cm^{-1} as a result of the reduction of Cu(II) to Cu(I).

Observation of all the features relevant for the “framework oxygen–cation–guest ligand” complexes $(\text{Si,Al})\text{O}_n\text{--M--L}_m$ in one IR experiment requires use of an extremely thin layer of a sample. Accordingly, under standard experimental arrangement, this requirement is hardly fulfilled and very often the spectral region between 1200 and 800 cm^{-1} has been omitted, because of the very strong intensity of the skeletal bands. Information on this region is usually obtained in an *ex-situ* experiment using a standard KBr technique. By employing FTIR technique and very thin self-supporting pellets ($\leq 5 \text{ mg/cm}^2$) of zeolites, such measurements in the above broad frequency range could be quite satisfactorily realized, with semiquantitative evaluation, but with exception of the region of the highly intensive antisymmetric band (1200–1000 cm^{-1}).

In this paper such an approach is applied on a model system of various divalent cations, Mn^{2+} , Mg^{2+} , Ni^{2+} , and Co^{2+} , exchanged into Na-ferrierites and using ammonia as a guest ligand. Measurements were done under conditions providing for a high reproducibility of the zeolite dehydration and ammonia adsorption/desorption procedure with various cation-exchanged ferrierites. The coverage of the cations by ammonia was estimated by measuring the intensity of the NH stretching (3400–3000 cm^{-1}) and bending regions (from 1600 to 1630 cm^{-1}). The response of the zeolite lattice (measured by the absorption changes at the skeletal region between 1000 and 400 cm^{-1}) to variation of the framework–cation and framework–cation–guest ligand bonding was monitored under strictly identical experimental conditions for all the metal ion-exchanged ferrierites.

2. Experimental Section

Materials. Metal ion-exchanged ferrierites were prepared by ion exchange of the Na form of ferrierite (TOSOH, with Si/Al 8.4) by using metal salt aqueous solutions. *Co-ferrierite* was prepared by cobalt exchange with 0.05 M cobalt acetate at 70 °C for 22 h. *Mg-ferrierite* and *Ni-ferrierite* were prepared by ion exchange using 0.5 M MgCl_2 and NiCl_2 , respectively, at 60 °C for 6 h. For *Mn-ferrierite* preparation the ion exchange with 0.05 M $\text{Mn}(\text{NO}_3)_2$ was applied. After the ion exchange the solids were thoroughly washed three times with distilled water, filtered, and then dried overnight in air at 80 °C. If

chloride solutions were used no traces of Cl^- ions were indicated in the last portion of the washing water. All the metal-loaded zeolites were then equilibrated with air humidity for 48 h.

The elemental analysis of zeolites after their dissolution was carried out by atomic absorption spectroscopy (AAS). The level of the metal ion expressed as M(II)/Al was 0.22 for Co, Mg, and Mn and 0.12 for Ni. The metal ion-exchange was carried out to reach approximately the degree of exchange of 50% of Na ions, but an even higher concentration of Ni salt solutions resulted in a lower degree of exchange for Ni.

FTIR Measurements. Infrared spectra were recorded in the 4000–400 cm^{-1} region at room temperature on a Magna-IR System 550 FTIR (Nicolet) spectrometer using a MCT-B liquid nitrogen cooled detector and equipped with a heatable cell (up to 500 °C) with NaCl windows connected to a vacuum system and a gas manifold.

Dehydration of zeolites was done by evacuation at increasing temperature (10 °C/min) with subsequent heating at 480 °C for 3 h. Ammonia adsorption (1 Torr) was carried out at room temperature on dehydrated samples, and its desorption was followed at evacuation for 30 min at temperatures between 150 and 480 °C. Ammonia was purified by a repeated freeze–pump–thaw technique and dosed into the system by keeping the temperature over condensed ammonia at –100 °C and thus the equilibrium pressure at 1 Torr. Under such conditions the adsorbed gas was free from water.

IR spectra were measured on zeolites in the form of self-supporting pellets (around 5 mg/cm^2) and normalized to a weight of 5.0 mg/cm^2 . Sample pellets were placed in a carousel sample holder providing for parallel positioning of up to six samples in the heated part of the cell and their sequential FTIR measurement. Thus a complete series of the samples presented here was measured in the same experimental run. Usually up to 300 scans were recorded at a resolution of 2 cm^{-1} for a single spectrum. The limit of the absorbance scale was usually over 2.5.

An exact background subtraction at the 1000–900 cm^{-1} region, i.e., with the bands emerging on the slope of the highly intensive antisymmetric T–O–T stretching band (which maximum runs over the limits of the absorbance scale), is difficult and would need a correct profile of the main antisymmetric T–O band at all desorption temperatures. We have found that the most reproducible and consistent results were obtained by constructing an individual background profile using spectra of the individual samples obtained prior to evacuation and their correction on the small shift of the main antisymmetric T–O band due to sample dehydration corresponding to the relevant profile of the parent Na-ferrierite measured under the same conditions. Overlapping bands were deconvoluted by using identification of the band maxima by a second derivative mode and the least-square minimalization routine approximating the bands by a Gaussian profile.

3. Results

The infrared spectra of Na-, CoNa-, NiNa-, MnNa-, and MgNa-ferrierites fully dehydrated by prolonged evacuation at 480 °C are shown in Figure 1, in the OH stretching and bending regions and the skeletal transmission window region, from 3700–1250 cm^{-1} and 980–800 cm^{-1} , respectively. To show the changes caused by zeolite dehydration, the spectra of hydrated and fully dehydrated Na- and CoNa-ferrierites are given in Figure 2. After zeolites are heated in vacuum at 480 °C, the infrared bands of adsorbed water both at the bending mode (around 1630 cm^{-1}) and at the stretching region (3700–

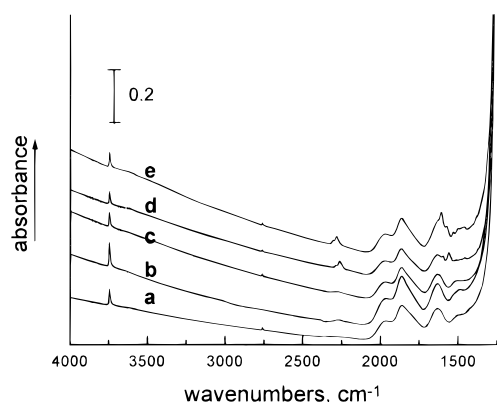


Figure 1. Infrared spectra of the dehydrated Na- (a), CoNa- (b), NiNa- (c), MnNa-, (d) and MgNa-ferrierite (e) after dehydration at 480 °C.

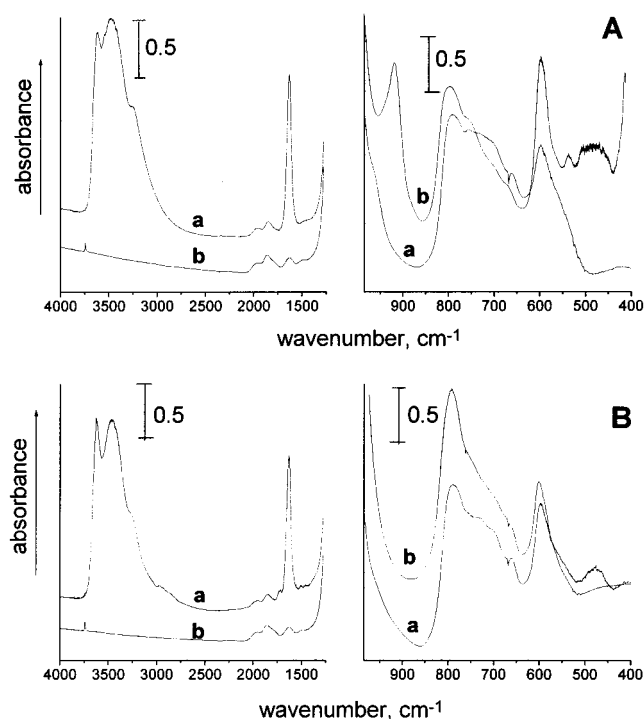


Figure 2. Infrared spectra of the CoNa- (part A) and Na-ferrierite (part B), hydrated (a) and after dehydration at 480 °C (b).

3000 cm^{-1}) present in hydrated samples diminished. The missing band of the stretching vibration of the bridging OH groups (at 3605 cm^{-1} for H-ferrierite) evidences the expected complete cationic form of the ferrierite. The small and narrow peak at 3745 cm^{-1} is assigned to the terminal Si–OH hydroxyls. The slightly higher, but still very low, intensity of Si–OH of CoNa-ferrierite is not significant and does not indicate structural collapse.

During dehydration of Na-ferrierite only a slight shift of the slope of the highly intensive main T–O antisymmetric band with a maximum at about 1070 cm^{-1} (according to measurements by the KBr technique) was observed in the transmission window between 980 and 800 cm^{-1} , but a new band structure appeared for the dehydrated M(II)Na-ferrierites (see Figures 1 and 2). In all cases the new band structures consisted of two components, both clearly displayed in the case of Mg- and Mn-ferrierites and less, but still apparent, in Co- and Ni-ferrierites (see deconvolution in Figure 3). The positions of the prominent low-frequency band for these cations (denoted as B_0) are summarized in Table 1. This band was taken as a base for evaluation of the framework–cation–guest ligand complexes (see below).

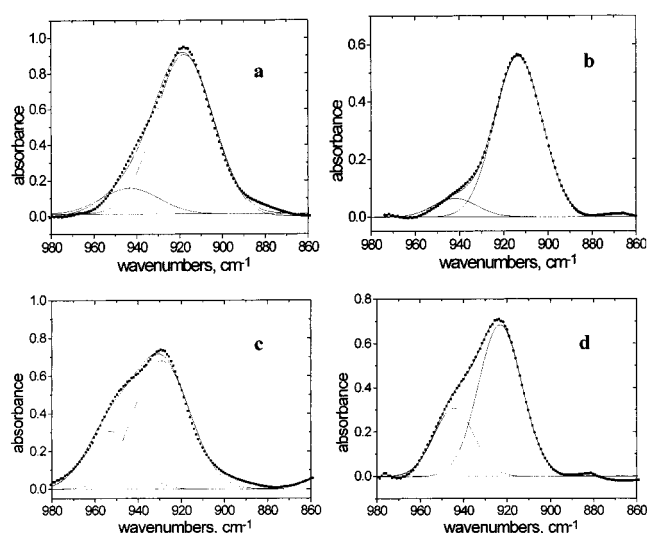
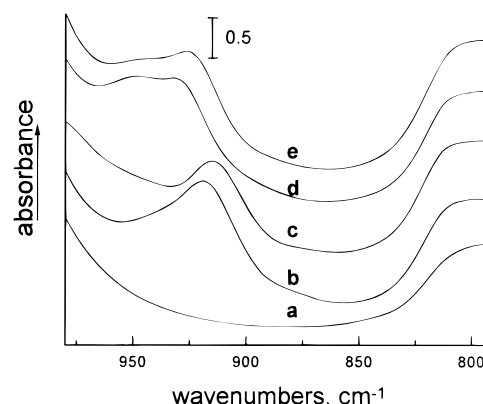


Figure 3. Deconvolution of the infrared spectra at the transmission window of CoNa- (a), NiNa- (b), MnNa- (c), and MgNa-ferrierite (d) after dehydration at 480 °C. Points, experimental data; lines, fitted spectra.

TABLE 1: Positions of the B_0 and B_1 Skeletal Bands for Metal-Exchanged Ferrierites without and with Adsorbed Ammonia, Respectively

metal cation	B_0 , cm^{-1}		B_1 , cm^{-1}
	main band	side band	
Mn(II)	927	953	951
Mg(II)	922	944	945
Co(II)	917	943	943
Ni(II)	913	943	943

The infrared spectra obtained after adsorption of ammonia and the following evacuation at increasing temperature for Na and metal exchanged zeolites are presented in Figures 4–8. (Notice here the reversed sequence of spectra a–e in two parts of the picture, given there for the graphic convenience of presentation.) In part b of Figures 5–8 is given a detail of the spectra in the 980–860 cm^{-1} region after background subtraction. In part c is depicted evaluation of the integral intensity changes as obtained by band analysis of the spectra for both NH stretching (3400–3000 cm^{-1}) and zeolite skeleton vibrations (bands B_0 and B_1). The infrared active NH modes observed for metal exchanged ferrierites with adsorbed ammonia (Figures 4–8) are summarized in Table 2. Positions of the new bands in the transmission window obtained in the spectra of ammonia adsorption/desorption on M(II)-ferrierites (denoted as B_1) are given in Table 1. No such presentation as in parts b and c of Figures 5–8 could be given for Na-ferrierite (Figure 4). The

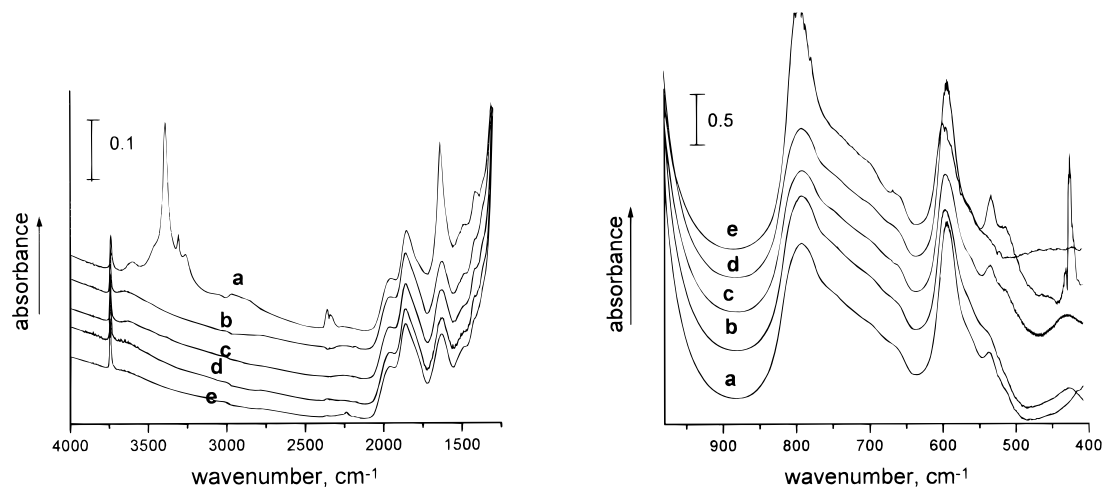


Figure 4. Infrared spectra of the dehydrated Na-ferrierite after 1 Torr of ammonia adsorption (a) and after its evacuation at 150 (b), 250 (c), 350 (d), and 480 °C (e).

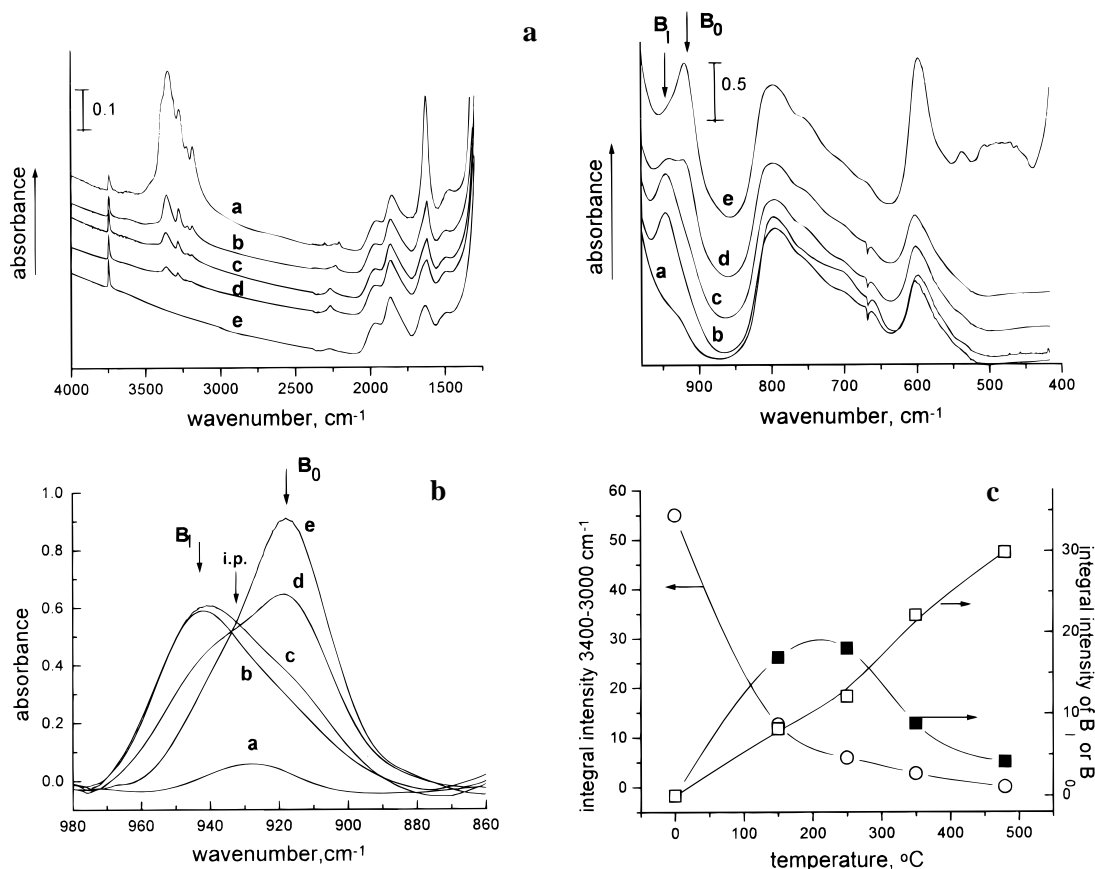


Figure 5. (a) Infrared spectra of the dehydrated CoNa-ferrierite after adsorption of 1 Torr of ammonia (a) and after its evacuation at 150 (b), 250 (c), 350 (d), and 480 °C (e). (b) Infrared spectra at the “transmission window” after background subtraction of the dehydrated CoNa-ferrierite after adsorption of 1 Torr of ammonia (a) and after its evacuation at 150 (b), 250 (c), 350 (d), and 480 °C (e). (c) Changes of the integral intensity of ammonia with increasing evacuation temperature in the region 3400–3000 cm^{-1} (○), and of the bands B_1 (■) and B_0 (○).

reason was that under the same procedure of spectra evaluation no bands could have been indicated on the low-frequency side of the antisymmetric T–O band of the Na-ferrierite.

Upon ammonia adsorption the band B_0 present in the transmission window of the M(II)Na-ferrierites disappeared and, with exception of a very small band at about 920–940 cm^{-1} , no other band was apparent on the low-frequency side of the highly intensive antisymmetric T–O band of ferrierite. Simultaneously, the strong bands in the NH stretching (3400–3000 cm^{-1}) and NH_3 bending (around 1640 cm^{-1}) regions evidenced a significant interaction of Na- and M(II)Na-ferrierites with

ammonia. During evacuation of the samples with adsorbed ammonia at elevated temperatures, an intensity decrease of the ammonia bands and, for M(II)Na-ferrierites, a parallel reappearance of new bands at the transmission window region occurred. A prolonged evacuation of the M(II)Na-ferrierites at 480 °C then led to complete recovery of all spectral features in the transmission window of the dehydrated zeolites observed prior to ammonia adsorption. Also the low-intensity band at about 920–940 cm^{-1} , observed with high ammonia coverage for all the M(II)Na-ferrierites, but absent for Na-ferrierite, diminished completely. These dominating characteristic changes

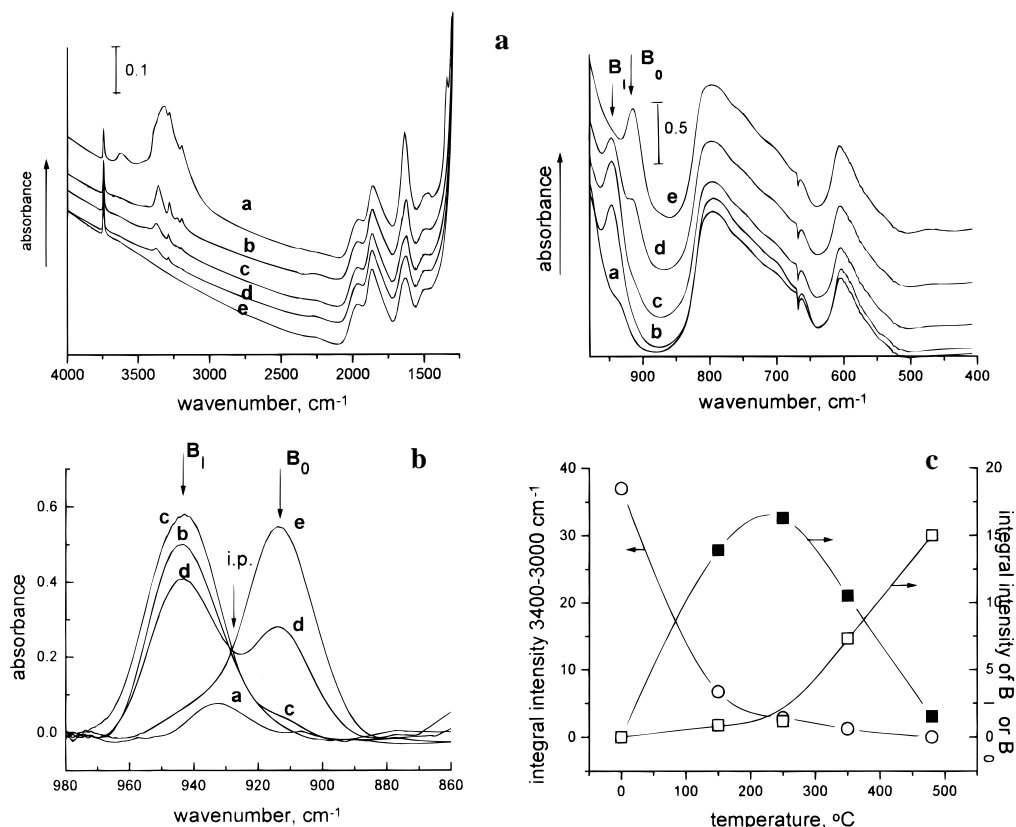


Figure 6. (a) Infrared spectra of the dehydrated NiNa-ferrierite after adsorption of 1 Torr of ammonia (a) and after its evacuation at 150 (b), 250 (c), 350 (d), and 480 °C (e). (b) Infrared spectra at the “transmission window” after background subtraction of the dehydrated NiNa-ferrierite after adsorption of 1 Torr of ammonia (a) and after its evacuation at 150 (b), 250 (c), 350 (d), and 480 °C (e). (c) Changes of the integral intensity of ammonia with increasing evacuation temperature in the region 3400–3000 cm⁻¹ (○) and of the bands B₁ (■) and B₀ (○).

observed at the transmission window were not accompanied by any systematic spectral changes in the 800–400 cm⁻¹ region.

The N—H stretching region of the spectrum of Na-ferrierite is dominated by a narrow band at 3390 cm⁻¹, accompanied by several less intensive peaks in the 3400–3000 cm⁻¹ region, and by a band at 1638 cm⁻¹ of the bending vibration (see Figure 4 and Table 2). However, upon evacuation of Na-ferrierite at 150 °C, all these bands diminished.

The spectra at the N—H stretching mode region of ferrierites containing both sodium and divalent cations, and measured in the presence of ammonia in the gas phase, consists of a superposition of peaks of ammonia bonded to Na and divalent cations (see Figures 5a–8a and Table 2). However, the spectra of M(II)Na-ferrierites measured after desorption at temperatures ≥ 150 °C could be assigned exclusively to ammonia interacting with a divalent cation.

Under various conditions of ferrierite treatment very low intensity bands with slightly changing profile and intensity were observed in the 2250–2310 cm⁻¹ region. Only the position of the main peaks for MgNa-ferrierite (2280 and 2303 cm⁻¹) and MnNa-ferrierite (2286 and 2263 cm⁻¹) could have been reasonably established. The intensity of the similar structures for other M(II)Na-ferrierites were below the experimental limits. Formation of a new species as a product of dehydration of the MgNa- and MnNa-ferrierite could be suggested, nevertheless we regard them as a minority features and they were not included in the discussion of the process of ammonia interaction with the metal-exchanged ferrierites. Thus the processes of ammonia adsorption and desorption could be accordingly described as follows: (i) Complete ammonia coverage of M(II)Na-ferrierites at ambient temperature results in diminishing of the band B₀ and only a small absorption appeared at 920–940 cm⁻¹. (ii) After

complete ammonia desorption a spectrum of the originally dehydrated ferrierite reappeared with identical B₀ band structure. (iii) By evacuation of M(II)Na-ferrierites with adsorbed ammonia at low temperatures an additional band (B₁) at 955–940 cm⁻¹ for the individual cations, together with the prominent band B₀, is present. (iv) The integral intensities of the B₀ and B₁ bands change in a regular manner for all the M(II)Na-exchanged ferrierites. Band B₁ predominates at the medium evacuation temperature and B₀ at the evacuation temperature above 400 °C. (v) The emergence and the integral intensity of the B₀ and B₁ bands correlates well with a decrease in the integral intensity of the bands of adsorbed ammonia. (vi) A single isosbestic point is observed between bands B₀ and B₁ by ammonia desorption.

It should be pointed out that the process of an interchange between B₀ and B₁ bands is more obvious for CoNa- and NiNa-ferrierite, where the B₀ band clearly predominates on dehydrated samples, while with MgNa- and MnNa-ferrierite a higher frequency side band accompanying the B₀ band in dehydrated zeolites coincides with the intensity of the B₁ band.

4. Discussion

The scheme of the discussion follows the order of the formation of the (Si,Al)O_n—M—(NH₃)_m complex, i.e., starting from the bare cation-framework interaction, continuing with a description of the cation–guest ligand interaction, and proceeding with analysis of the framework–cation–guest ligand complex.

4.1. Bare Cation–Framework Interaction. The B₀ band is ascribed to the effect of the cation on the antisymmetric stretching mode of the part of T—O—T bonds adjacent to the

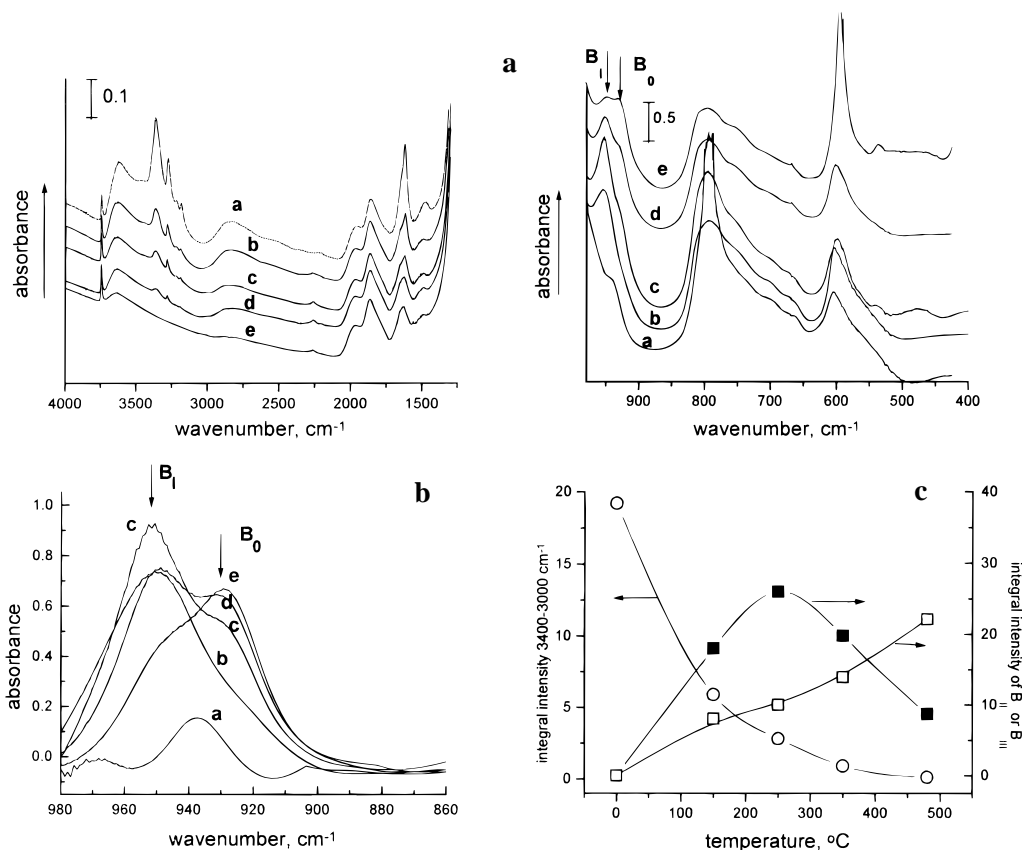


Figure 7. (a) Infrared spectra of the dehydrated MnNa-ferrierite after adsorption of 1 Torr of ammonia (a) and after its evacuation at 150 (b), 250 (c), 350 (d), and 480 °C (e). (b) Infrared spectra at the “transmission window” after background subtraction of the dehydrated MnNa-ferrierite after adsorption of 1 Torr of ammonia (a) and after its evacuation at 150 (b), 250 (c), 350 (d), and 480 °C (e). (c) Changes of the integral intensity of ammonia with increasing evacuation temperature in the region 3400–3000 cm^{-1} (○) and of the bands B_1 (■) and B_0 (□).

cation and shifted from the position at about 1070 cm^{-1} to lower frequencies and is interpreted as local perturbation of the framework produced by divalent metal ion bonding to framework oxygens. In the broad and high intensity antisymmetric stretching band of the unperturbed T–O–T bonds at about 1070 cm^{-1} , the Si–O–Si and Si–O–Al vibration could not be distinguished, as similarly claimed by Datka et al.¹⁸ The interpretation of B_0 is based on the theoretical background given by van Santen¹⁴ and experimental data provided for Co–, Cu–Ni–Y,¹⁷ Cu–ZSM-5,^{19–21} and Co–ZSM-5¹⁰ zeolites.

By evaluation of the position of the prominent band B_0 , prevailing after M(II)Na-ferrierite dehydration at 480 °C (see Table 1) and connected with the location of a bare cation at the zeolite cationic sites, the following order of the shift to lower wavenumbers for various divalent metal ion-exchanged ferrierites has been obtained:



The difference of the B_0 band maxima for the individual metal cations is at least 4 cm^{-1} (i.e., the difference between the value for Ni- and Co-ferrierite), and despite a half-width of the band of about 25–30 cm^{-1} , the sequence has been reproducibly established in repeated experiments.

The accompanying high frequency side band of the prominent B_0 peak, displayed more in MnNa- and MgNa-ferrierites, could be assigned to a cation environment causing lower local framework perturbation. Such a decrease in the effect of the cation bonding could be caused by a change in coordination of framework oxygens to a metal cation or by a lower strength of the cation complexation ability. Generally, it could be caused

also by a decrease of the formal charge on the cation or, as discussed below, by the presence of an external ligand. As no extra ligand was unequivocally identified in the spectra after prolonged evacuation at 480 °C, the last interpretation would be excluded. The stability of the divalent state of the studied cations in zeolites is well-known;^{22,23} moreover, the observed profile of the B_0 band did not change after oxidation in oxygen (100 Torr, 450 °C). Accordingly, it ruled out the explanation for the B_0 side bands as a decrease of the formal oxidation state of the exchanged cations. We propose bonding of the metal ions at different cationic sites of the zeolite as a reason for the observed side bands at the B_0 band position.²³

The extent of local perturbation of the lattice increases with increasing value of the shift of the B_0 band with respect to the unperturbed T–O–T antisymmetric stretching mode of the parent hydrated Na-ferrierite at 1070 cm^{-1} , accordingly the lattice deformation decreases from Ni to Mn cation. It should be mentioned that the position of the band at 1070 cm^{-1} is a value obtained in measurements by a standard KBr technique, thus on a sample equilibrated with air humidity. As indicated by a small shift of the position of the slope of the main T–O–T antisymmetric band during dehydration, some shift of the maximum of 1070 cm^{-1} is possible during the zeolite treatment. Nevertheless, as we have no measurements available at this region on dehydrated samples, the value of 1070 cm^{-1} was used as the reference.

The obtained order of (1) reflects the degree of the local perturbation of the lattice and accordingly the order of the strength of the bonds of the individual bare cations to the framework oxygen ligands. Obviously the cation–framework

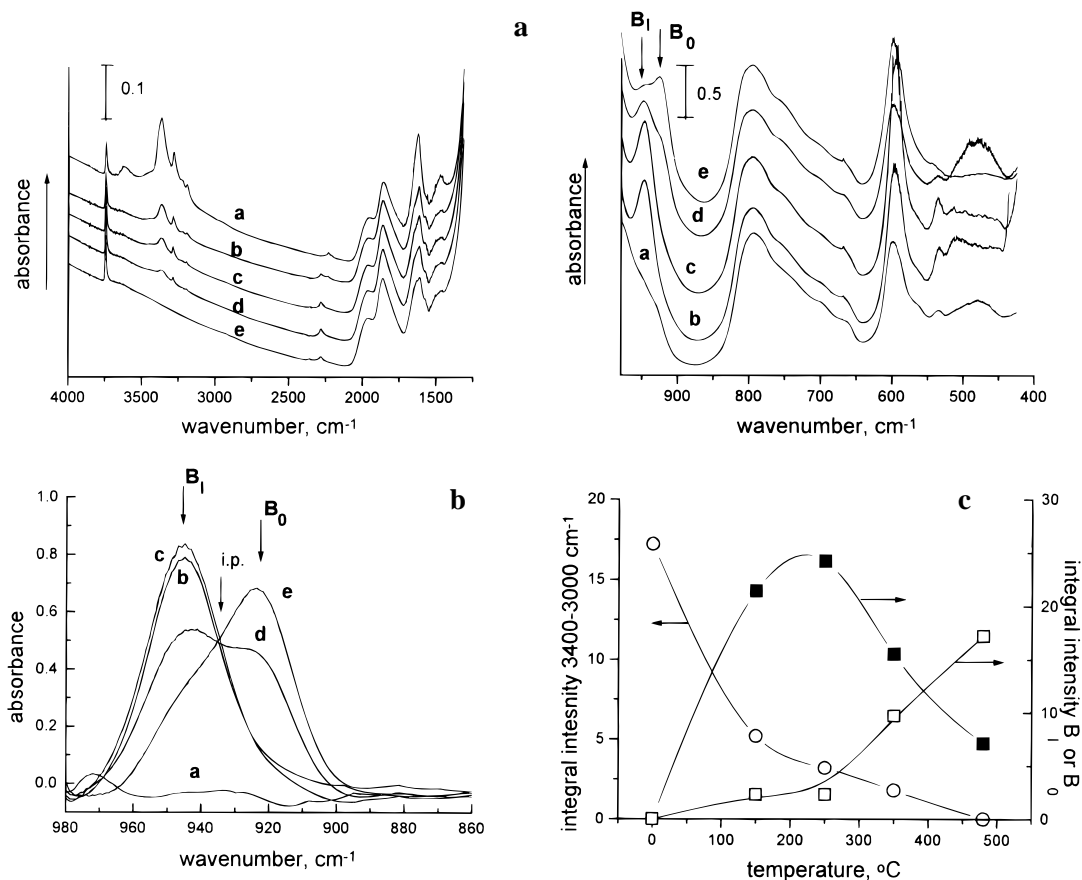


Figure 8. (a) Infrared spectra of the dehydrated MgNa-ferrierite after adsorption of 1 Torr of ammonia (a) and after its evacuation at 150 (b), 250 (c), 350 (d), and 480 °C (e). (b) Infrared spectra at the “transmission window” after background subtraction of the dehydrated MgNa-ferrierite after adsorption of 1 Torr of ammonia (a) and after its evacuation at 150 (b), 250 (c), 350 (d), and 480 °C (e). (c) Changes of the integral intensity of ammonia with increasing evacuation temperature in the region 3400–3000 cm^{-1} (○), and of the bands B_1 (■) and B_0 (□).

TABLE 2: Infrared Active Modes of N–H Observed for Ammonia on M(II)Na-ferrierites after Ammonia Desorption at 150 °C

metal ion	N–H vibrations, cm^{-1}				
	3359(s)	3280(s)	3214(w)	3186(w)	1618
Mn(II)	3363	3285	3222	3194	1625
Co(II)	3357	3281	3219	3192	1624
Ni(II)	3360	3280	3223	3194	1635

^a s, strong band; w, weak peak. After adsorption of 1 Torr of ammonia on Na-ferrierite at room temperature infrared active N–H modes were identified at 3391(s), 3309(w), 3457(sh), 3262(sh), and 1638 cm^{-1} . These bands disappeared after desorption at 150 °C.

oxygen bonding should parallel the stability of similar oxygen ligand complexes, but an additional effect of confinement of the complex in the electrical field of the zeolite channels cannot be omitted. It has been expected that the local lattice perturbation could be correlated with cation radius and electronegativity (see, e.g., ref 17). The ion radius of the six-coordinated ions increases from Mn^{2+} (67 pm), to Mg^{2+} (72 pm), to Co^{2+} (74.5 pm), as well as the shift of the B_0 band position (relative to 1070 cm^{-1}) (cf. Table 1). Nevertheless, the ion radius of Ni^{2+} (69 pm) would be consistent with a B_0 position similar to that of Mn, but the position of the B_0 band for Ni-ferrierite is shifted even to lower wavenumbers than for the Co ion (radius 74.5 pm). On the other hand, a linear correlation was obtained between shifts of the B_0 positions and heat of hydration, increasing in the sequence of Mn^{2+} (655 kcal/mol), Co^{2+} (696 kcal/mol), Ni^{2+} (716 kcal/mol) cations, a value directly related to the stability of cation aquocomplexes.²⁴ The sequence (1) is also in good correlation with the decrease of the total

stabilization energies, calculated by Klier¹⁵ for various divalent cations in zeolite oxygen six-ring windows, and decreases from Ni to Mn, i.e., $\text{Ni} > \text{Co} > \text{Mn}$.

4.2. Bare Cation–Guest Ligand Interaction. To analyze the spectra of the ammonia adsorption on M(II)Na-zeolites, two possible adsorption modes should be generally considered, i.e., (i) formation of metal ammine complexes and (ii) ammonia dissociative adsorption.

Dissociative adsorption should lead to a negatively charged ligand (NH_2^-) bonded to the cation and formation of an OH group. Really, a limited extent of dissociative adsorption is supported by the appearance of a small broad band at about 3610 cm^{-1} , i.e., close to the frequency of the H-ferrierite structural hydroxyls (3605 cm^{-1}), accompanied by a very weak band at about 1470 cm^{-1} , assigned to NH_4^+ ion. Nevertheless existence of a bridging OH group in the presence of the gas phase ammonia at room temperature is hardly acceptable and would then indicate an OH group of very low acidity, such as M–OH. Both the previously indicated features diminish after evacuation above 150 °C. The position of the N–H stretching bands of the NH_2 species might be expected²⁵ to be at about 3200 and 3150 cm^{-1} , however, these bands could not be identified unequivocally in the complex profile of the 3400–3000 cm^{-1} region. Accordingly, we assume that ammine complexes prevail on M(II)Na-ferrierites evacuated at temperatures above 150 °C, and, due to low stability of ammonia adsorption on Na-ferrierite, all the bands in the 3400–3000 cm^{-1} region evacuated above 150 °C should be assigned exclusively to stretching modes of $\text{M(II)}-(\text{NH}_3)_n$ complexes.

Ammine complexes containing exclusively NH_3 ligands in

the first coordination sphere are expected by theory to display only two characteristic bands of antisymmetric and symmetric stretching vibration modes in the 3400–3000 cm^{-1} region.^{25,26} On the other hand, as depicted in Figures 4–8 and summarized in Table 2, the spectra of M(II)Na-ferrierites with partially covered ammonia reflect two prominent bands around 3360 and 3280 cm^{-1} and two less intensive bands at 3220 and 3190 cm^{-1} . The position of these bands is slightly influenced by a type of divalent cation but changes less with ammonia coverage. As already mentioned, the intensity ratio of the individual components of the complex spectrum does not change markedly with the decreasing NH_3 coverage upon evacuation above 150 °C.

Such complexity of the spectra of ammine complexes in the N–H stretching region, noticed already for other metal ammine complexes embedded in zeolites (e.g., four bands for $\text{Cu}(\text{NH}_3)_4$ in CuY^{27}), could be attributed to several aspects specific for the presence of a metal–ligand complex in zeolite cavities. It can correspond to (i) formation of mixed complexes, containing both a guest molecule and framework oxygens as metal ion ligands, (ii) variation of the metal ion siting in the zeolite and/or change of the charge on the metal cation, and (iii) a spatial restriction enforced on the metal ion–ammine complex by the inner volume of the zeolite cavities/channels and leading to a decrease in symmetry of the $\text{M}(\text{NH}_3)_n$ complex. It should be noted that the summary profile in the 3400–3000 cm^{-1} region could be further complicated by a band at about 3200 cm^{-1} of the 2 δ_{as} (HNH) or due to Fermi resonance of one N–H stretching mode with 2 δ_{as} (HNH).²⁶

A detailed analysis of the complex spectra in the 3400–3000 cm^{-1} region is beyond the scope of this study. Nevertheless, it can be concluded that catio–ammine complexes prevail on M(II)Na-ferrierites at higher evacuation temperatures. Accordingly, the integral intensity of the complex band at 3400 and 3000 cm^{-1} could be taken as a measure of the cation coverage by ammonia and thus the number of ammine complexes present.

4.3. Framework–Cation–Guest Ligand Interaction. The process of ammonia desorption at increased temperature would be described as decomposition of $\text{M}(\text{NH}_3)_n$ ammine complexes. At high ammonia coverage, high ammine complexes ($n = 4$ –6) can be present, e.g., $\text{Cu}(\text{NH}_3)_4$ was found in Y-zeolite.²⁷ Such complexes are assumed to be constrained only by intrazeolite volume and demands on the charge compensation and are formed with a very limited participation of framework oxygens. At low ammonia coverage these mixed framework–cation–guest ligand complexes decompose into the monoammine ligand structure of $(\text{Si,Al})\text{O}_n\text{--M--NH}_3$ and eventually bring about formation of a bare cation at the cationic sites, $(\text{Si,Al})\text{O}_n\text{--M}$, bonded to framework oxygens. The process of a competition between the framework oxygen ligands and the guest ligands for cation coordination and going through a 1:1 complex as the terminal structure containing the guest molecule, before formation of a bare cation, is well documented in the literature.^{14,15,17,18,28,29}

The existence of a relatively low intensity peak in the 920–940 cm^{-1} region on highly ammonia covered ferrierites probably holds an interesting information on accommodation of the cation polyammonia complexes in the ferrierite channels. (Notice that such a broad band at about 960 cm^{-1} with low intensity is also seen in the highly hydrated sample of CoNa-ferrierite containing $[\text{Co}(\text{H}_2\text{O})_6]^{2+}$ complexes;¹⁵ see Figure 2, part A, spectrum a.) However, evaluation of these peaks of very low intensity is above the possibilities of the experimental data presented here.

Observation of a single isosbestic point during the deamination process indicates the existence of a single equilibrium

between structures represented by the infrared bands denoted as B_1 and B_0 (see Figure 5b–8b). It could be reasoned that one partner of the equilibrium includes the structure of the ferrierite lattice perturbed due to bonding of a bare cation to the framework oxygen ligands (band B_0), produced by complete zeolite dehydration at 480 °C. The second component (B_1) could be then assigned to the cation interacting less strongly with the lattice oxygens, owing to its simultaneous bonding to ammonia, i.e., forming $\text{M}(\text{II})\text{--}(\text{NH}_3)_n$. There is little doubt that this is a complex with the lowest value of n , which is formed during decomposition of a higher $\text{M}(\text{II})\text{--}(\text{NH}_3)_n$ species prior to release of all ammonia and formation of the bare cation. This has led us to assignment of the species represented by B_1 to the $\text{M}(\text{II})\text{--NH}_3$ 1:1 complex.

Additional arguments are as follows: (i) a general correlation exists between the decrease of the guest molecule coverage and the intensity changes of both the B_1 and B_0 bands, e.g., at the region of low ammonia coverage (see Figures 5c–8c); (ii) the maximum of the B_1 intensity at the increasing temperature of desorption is reached under conditions where the content of the adsorbed ammonia (evaluated from an intensity decrease of the N–H stretching band) decreased to a value below ca. 20% of the full saturation for the individual cations (Figures 5c–8c). Assuming formation of a complex with $n = 4$ (as found in CuY^{27}) or even a complex with the maximum coordination number of 6 for a metal cation highly saturated by ammonia, such a decrease in intensity of the N–H stretching bands is consistent with the previous interpretation of the last complex species composition as the $\text{M}(\text{II})\text{--NH}_3$ 1:1 complex.

The quantitative aspect of the integral intensity of the skeletal B_1 and B_0 bands is indicated by a good correlation between the sum of the intensity of the B_1 and B_0 bands for zeolites evacuated at elevated temperatures and the M(II)/Al composition (see Figures 5c–8c). From this information, it is suggested that the integral intensity of the B_1 and B_0 bands could be used for semiquantitative evaluation of the amount of bare cations and the proposed 1:1 cation–guest ligand complexes (cf. Sárkány and Sachtler,¹⁹ who showed correlation of the intensity of the band of the $\text{Cu}(\text{I})\text{--CO}$ complex with that of the corresponding T–O–T skeletal band).

This implies that Figures 5c–8c could be understood as representing variations in the abundance of the bare cation and the proposed 1:1 cation–guest ligand complex under changing ammonia coverage. Accordingly, the temperature of the maximum of the curves indicates the relative stability of such a cation–ligand complex and the height of this maximum the abundance of this component at the equilibrium during desorption. The ratios of the integrated areas for the bands B_0 and B_1 must bear some important information on the process of ammine complex formation in the M(II)Na-ferrierites. Their variations with temperature give an insight into the relative stabilities of the $\text{M}(\text{II})\text{--NH}_3$ complexes embedded in ferrierite. These data were evaluated by calculating a distribution coefficient, δ_{ML} , given as a ratio of the amount of the M--NH_3 complexes to the total metal content. Supposing that the integral intensity of the B_0 and B_1 bands is proportional to the number of the bare M(II) ions and the $\text{M}(\text{II})\text{--NH}_3$ complexes, respectively, the $\delta_{\text{ML}} = [\text{M}(\text{II})\text{--NH}_3]/c_{\text{M}}$ could be taken as equal to the ratio of the integral intensity of the B_1 band at a given temperature to the integral intensity of the B_0 band after complete ferrierite dehydration. Therefore, after ammonia evacuation at 250 °C the values of δ_{ML} for CoNa- and NiNa-ferrierites were 0.46 and 0.98, respectively. This implies that under identical desorption temperature, the order of the relative abundance of

the $(\text{Si,Al})\text{O}_n\text{--M--NH}_3$ complex in equilibrium with the $(\text{Si,Al})\text{O}_n\text{--M}$ bare cation in $\text{M(II)Na-ferrierites}$ follows roughly the order expected from the values of the stability constants for the metal-ammine complexes given in ref 26, i.e., $\text{Ni} > \text{Co}$. To evaluate the same parameter for MnNa- and MgNa-ferrierite is dubious because of coincidence of the proposed 1:1 cation–ammine complex with the higher frequency sideband to the dominating band B_0 induced by a bare cation.

5. Conclusions

The FTIR measurements at the “transmission window” around 900 cm^{-1} have shown the possibility to distinguish between the local lattice perturbation produced by the bare divalent cations and those from the divalent cations bearing ammonia as an extraframework ligand.

The presence of a bare divalent metal ion (Mn^{2+} , Mg^{2+} , Ni^{2+} , and Co^{2+}) at the cationic sites of dehydrated ferrierite causes local perturbation of the adjacent T–O–T, as evidenced by the changes in the T–O–T framework vibrations. A new band appearing at the “transmission window” between 980 and 860 cm^{-1} represents a fraction of the ferrierite framework influenced by the presence of a divalent cation and is assigned, in accordance with the previous interpretation of similar systems,^{17,19–21} to the T–O–T antisymmetric stretching vibration mode of the perturbed zeolite framework. The value of a shift, using for convenience the position of the unperturbed T–O–T antisymmetric stretching band in hydrated sample as reference, is related to the change of the T–O–T angle and so the degree of the local deformation of the lattice caused by the vicinity of the divalent cation. Thus the framework perturbation increases in the following order: $\text{Ni} > \text{Co} > \text{Mg} > \text{Mn}$.

The extent of the above described perturbation of the zeolite lattice is partly removed when an extraframework ligand is bonded to the cation. The reverse shift of the perturbed T–O–T antisymmetric band produced by bonding of an external ligand (ammonia) to the divalent cation amounts to about one-fifth of the effect produced by a bare cation alone.

Both these findings, enabling one to distinguish the effect of a divalent bare cation $(\text{Si,Al})\text{O}_n\text{--M}$ and of cation–guest ligand complexes $(\text{Si,Al})\text{O}_n\text{--M--NH}_3$ on the adjacent T–O–T framework deformation together with monitoring of the adsorbed molecules, shows that FTIR spectroscopy has a potential for highly sensitive identification of equilibrium states between the bare metal ions and metal ion–ligand complexes in zeolites. Moreover, it seems promising to employ this approach in order to distinguish siting of divalent cations in zeolites and eventually to carry out *in situ* investigations on the framework–cation–guest ligand interactions under conditions close to real catalysis.

Note Added in Proof. It has recently been shown^{30–32} that the local perturbation effect of the Cu(I) ion in ZSM-5 on the antisymmetric T–O–T lattice mode was altered by Cu(I) complexation with CO or molecular oxygen as external guest

ligands. Thus, while the single Cu(I) ions caused a shift of the internal asymmetric T–O–T vibration to about 966 cm^{-1} ,²⁰ the band appeared at $995\text{--}988\text{ cm}^{-1}$ after saturation of Cu(I) with CO .³²

Acknowledgment. We are grateful for financial support of the Grant Agency of the Czech Republic (Project No. 203/96/1089) and of Air Products & Chemicals, Inc., PA. Help of the reviewers in improvement of the final version of this manuscript is greatly appreciated.

References and Notes

- (1) Iwamoto, M.; Yahiro, M. *Catal. Today* **1994**, 22, 5.
- (2) Amiridis, M. D.; Zhang, T.; Farrauto, R. *J. Appl. Catal. B: Environ.* **1996**, 10, 203.
- (3) Sullivan, J. A.; Cunningham, J.; Morris, M. A.; Keneavey, K. *Appl. Catal. B: Environ.* **1995**, 7, 137.
- (4) Schoonheydt, R. A. *Catal. Rev.-Sci. Eng.* **1993**, 35, 129.
- (5) Calligaris, M.; Nardin, G.; Randaccio, L. *Zeolites* **1984**, 4, 251.
- (6) Calligaris, M.; Mezzetti, A.; Nardin, G.; Randaccio, L. *Zeolites* **1986**, 6, 137.
- (7) Calligaris, M.; Mezzetti, A.; Nardin, G.; Randaccio, L. *Zeolites* **1985**, 5, 317.
- (8) Dooryhee, E.; Greaves, G. N.; Steel, A. T.; Townsend, R. P.; Carr, S. W.; Catlow, C. R. *Faraday Discuss. Chem. Soc.* **1990**, 89, 119.
- (9) Esemann, H.; Foerster, H.; Geidel, E.; Krause, K. *Microporous Mater.* **1996**, 6, 321.
- (10) Sun, T.; Trudeau, M. L.; Ying, J. Y. *J. Phys. Chem.* **1996**, 100, 13662.
- (11) Lamberti, J. C.; Bordiga, S.; Salvalaggio, M.; Spoto, G.; Zecchina, A.; Geobaldo, F.; Vlaic, G.; Bellatreccia, M. *J. Phys. Chem. B*, **1997**, 101, 344.
- (12) Dědeček, J.; Sobalík, Z.; Tvarůžková, Z.; Kaucký, D.; Wichterlová, B. *J. Phys. Chem.* **1995**, 99, 16327.
- (13) Wichterlová, B.; Dědeček, J.; Sobalík, Z.; Vondrová, A.; Klier, K. *J. Catal.* **1977**, 169, 194.
- (14) van Santen, R. A.; Vogel, D. L. *Adv. Solid-State Chem.* **1989**, 1, 151.
- (15) Klier, K. *Langmuir* **1988**, 4, 13.
- (16) Koningsberger, D. C.; Miller, J. T. In *Zeolites: A Refined Tool for Designing Catalytic Sites*; Stud. Surf. Sci. Catal. **1995**, 97, 125.
- (17) Jacobs, W. P. J. H.; van Wolput, J. H. M. C.; van Santen, R. A. *Zeolites* **1993**, 13, 170.
- (18) Datka, J.; Geerlings, P.; Mortier, W.; Jacobs, P. A. *J. Phys. Chem.* **1985**, 89, 3483.
- (19) Sárkány, J.; Sachtler, W. M. H. *Zeolites* **1994**, 14, 7.
- (20) Lei, G. D.; Adelman, B. J.; Sárkány, J.; Sachtler, W. M. H. *Appl. Catal. B: Environ.* **1995**, 5, 245.
- (21) Sárkány, J.; Sachtler, W. M. H. *Catalysis by Microporous Materials. Stud. Surf. Sci. Catal.* **1995**, 94, 649.
- (22) Wichterlová, B.; Jirů, P.; Cufínová, A. Z. *Phys. Chem. N. F.* **1974**, 88, 180. Wichterlová, B.; Beran, S.; Bednářová, S.; Nedomová, K.; Jirů, P. *Innovation in Zeolite Materials Science. Stud. Surf. Sci. Catal.* **1988**, 37, 199.
- (23) Sobalík, Z.; Wichterlová, B. *Book of Abstracts of the EUROPACAT-III*; Krakow, **1997**; p 464. Dědeček, J.; Wichterlová, B. *Ibid.*; p 398.
- (24) Schlaefer, H. L.; Gliemann, G. *Ligand Field Theory*, Wiley-Interscience: London, 1969.
- (25) Nakamoto, K. *Infrared and Raman Spectra of Inorganic Coordination Compounds*; Wiley-Interscience: New York, 1977; pp 197–204.
- (26) Schmidt, K. H.; Mueller, A. *Coord. Chem. Rev.* **1976**, 19, 41.
- (27) Howard, J.; Nicol, J. M. *J. Chem. Soc., Faraday Trans. 1*, **1989**, 85, 1233.
- (28) Riley, P. E.; Seff, K. *Inorg. Chem.* **1974**, 13, 1355.
- (29) Kubelková, L.; Wichterlová, B. *Coll. Czech. Chem. Commun.* **1977**, 42, 2033.
- (30) Sárkány, J. *J. Mol. Struct.* **1997**, 410–411, 95.
- (31) Sárkány, J. *J. Mol. Struct.* **1997**, 410–411, 137.
- (32) Sárkány, J. *J. Mol. Struct.* **1997**, 410–411, 145.